Experimental Confirmation of Ponderomotive-Force Electrons Produced by an Ultrarelativistic Laser Pulse on a Solid Target

G. Malka and J. L. Miquel

Commissariat à l'Energie Atomique, Centre d'Etudes de Limeil-Valenton, 94195 Villeneuve-Saint-Georges, Cedex, France

(Received 25 March 1996)

First measurements of relativistic electrons produced by the interaction between a 400-fs, 1.06-μm ultrahigh-intensity laser pulse ($I > 10^{19}$ W/cm^2) and a solid target are presented. For electrons ejected along the laser propagation axis in the forward direction, the relation of the hot temperature T_h versus the laser intensity I is found to be in very good agreement with a $\mathbf{J} \times \mathbf{B}$ ponderomotive model described by S. C. Wilks *et al.* [Phys. Rev. Lett. **69**, 1383 (1992)], where $T_h = (\gamma_{\rm osc} - 1)mc^2$. Hot temperature of transverse electrons scales as $T_h \sim I^{1/3}$. [S0031-9007(96)00479-6]

PACS numbers: 52.40.Nk

Recent observations of MeV electrons escaping from plasma have been made on high-intensity picosecond interactions with solid targets or preformed plasma [1], and a pulsed gas jet [2]. The production of energetic electrons with a high efficiency, particularly in the laser propagation direction, requires ultraintense laser pulses. The fast ignitor concept [3], relevant to the inertial confinement fusion (ICF) studies, enhances the interest to investigate the generation of energetic electrons produced by this interaction. Several mechanisms can produce high-energy electrons. For laser intensities higher than 10^{18} W/cm^2, electrons trapped by the ponderomotive potential become relativistic. Particle-in-cell (PIC) simulations have shown that the laser pulse should make a hole in overdense plasmas by ejecting matter from high laser intensity regions of the focal spot [4]. A characteristic parameter is the classical normalized momentum of electrons quivering in the laser electric field: $a = p_{\rm osc}/mc = eE/m\omega_0 c = 8.53 \times 10^{-10} \times (I\lambda^2)^{1/2}$, where e is the electron charge, E is the magnitude of the laser field at focus, m is the electron mass, ω_0 is the laser angular frequency, c is the speed of light, I is the laser intensity in W/cm^2, and λ is the laser wavelength in microns. At a laser intensity equal to 2×10^{19} W/cm^2, a is approximately equal to 4, defining an ultrarelativistic regime. For $a < 1$, i.e., $I\lambda^2 < 10^{18}$ W/cm^2 μm^2, electrons are ejected from the laser focus where the electric field is maximum by the radial component of the ponderomotive force $\mathbf{F_r} = -(e^2/2m\omega_0^2)\Delta_{\mathbf{r}}\langle E^2\rangle$. This force accelerates the electrons in the perpendicular direction over many microns. For $a > 1$, the laser magnetic field is no longer negligible, and the longitudinal component of the Lorentz force $-e\mathbf{v} \times \mathbf{B}$ expels the electrons in the longitudinal direction. For a short density gradient scale length $L < \lambda$ (where $1/L = \Delta n/n$, and n is the electron density), electrons escape from the laser field in a single optical cycle with a kinetic energy $W_{\rm osc}$, given by the ponderomotive potential, $W_{\rm osc} = (\gamma_{\rm osc} - 1)mc^2$, with $\gamma_{\rm osc} = 1/[1 - (v/c)^2]^{1/2} = (1 + a^2)^{1/2}$. Wilks *et al.* [4] have performed PIC numerical experiments of the interaction of an intense picosecond laser pulse with a solid target. The energetic electron distribution is described by a Boltzmann distribution $f(W) = dN/dW \sim \exp(-W/kT_h)$, where k is the Boltzmann constant, and T_h is defined as the hot electron temperature. kT_h is found to be equal to $W_{\rm osc}$. Then, T_h (MeV) is of the order of $0.511[(1 + I_{18}/1.37)^{1/2} - 1]$.

Other mechanisms are also responsible for energetic electron production. At the critical density n_c (n_c approximately equal to 10^{21} cm^{-3} for a 1 μm laser wavelength), resonant absorption occurs for a p polarization radiation, and generates strong longitudinal electrostatic fields. These electrostatic fields accelerate energetic electrons in the longitudinal direction [5]. Parametric instabilities such as the ion-acoustic decay (IAD), in a nonlinearly steepened density profile, produce hot electrons in the transverse direction at the critical density [6]. Simulation results show that the hot temperature of the electron distribution scales as $(I\lambda^2)^{1/3}$, and reaches 100 keV for $I\lambda^2 = 10^{18}$ W/cm^2 μm^2. The fraction of the incident laser light energy absorbed into the hot electron tail is typically (10–20)% [6]. For lower electron densities $n_e < n_c/4$, the exponential growth rate of the Raman instability is well known [7], and the saturation of this instability appears quickly. Electron plasma waves are amplified by the Raman effect and are no longer sinusoidal in the relativistic regime. This "wave breaking," observed experimentally by Modena *et al.* [2] in laser-gas interactions at $I\lambda^2 \sim 10^{18}$ W/cm^2 μm^2, generates relativistic plasma oscillations, and accelerates energetic electrons to over 40 MeV in the laser propagation direction. For such conditions, relativistic self-channeling has been studied and observed in laser-gas interactions at $I\lambda^2 > 10^{18}$ W/cm^2 μm [8], for laser powers higher than a few terawatts in a 10^{19} cm^{-3} electron density plasma. The laser beam is focused over two Rayleigh lengths, and the focused intensity is assumed to be multiplied by 15. Electrons are also ejected radially from the channel by a strong ponderomotive force. MeV electrons from

picosecond laser-plasma interaction have been detected directly by Darrow *et al.* [1]: The hot temperature was found to be equal to 1 MeV for a 10^{18} W/cm^2 laser intensity. The laser intensity contrast ratio was 1000:1, producing a long density gradient scale length ($L \sim 10-30$ μm), so Raman scattering was probably the dominant effect producing these electrons. Indirect experimental electron studies have also been done by measuring energetic ions [9] and hard x rays [10]. X-ray emission shows the plasma confinement by the nonrelativistic ponderomotive force ($I\lambda^2 < 10^{18}$ W/cm^2 μm) by measuring the Li-like satellites of an Al-solid density plasma [11].

In this Letter, we present direct measurements of MeV electron distributions produced by the interaction of an intense subpicosecond and high intensity contrast ratio laser pulse with a solid target. We study the hot temperature evolution of the electron distribution versus the laser intensity for two kinds of irradiation and three observation angles.

The experiments described here were performed with the 80 TW P102 laser system [12] at CEA/LV. The laser produces pulses with the following characteristics: $\lambda_{\text{laser}} = 1.056$ μm, E_{laser} up to 40 J, $\tau_{\text{laser}} = 300-500$ fs, I_{laser} up to 2×10^{19} W/cm^2. The laser beam was focused either with a $f/3$ off-axis parabola or on-axis parabola, with s or p polarizations. The focal spot has a 10 μm diameter, containing approximately 10% of the laser energy. The remainder is localized in a very large surface and then do not contribute to the production of hot electrons. The intensity contrast ratio (pulse shape) was measured, and reached 10^8:1, a few tens of ps before the 300 fs pulse. The density gradient scale length calculated by the CHIVAS [13] hydrodynamic code was of the order of the laser wavelength. This performed a near critical electron density interaction. Energetic electron distributions from 0.06 to 3 MeV were measured directly with two electron spectrometers. Two experiments were performed: in experiment A, the laser beam was focused by a $f/3$ off-axis parabola onto a 30 μm thick CH target, at normal incidence (see Fig. 1). The maximum laser intensity was varied from 10^{18} to 10^{19} W/cm^2 by increasing the laser energy. Electrons were detected by a 0.4–3 MeV spectrometer along the laser propagation axis in the forward direction and at 22° to this axis in the forward direction. In experiment B, the focalization of the laser beam was realized by a $f/3$ on-axis parabola, onto a massive silicate target, with a 45° incidence angle. We performed this experiment with both s and p polarizations. Energetic electron distributions from 0.06 to 1.1 MeV ejected along the target surface, at 135° of the laser axis in the backward direction, were measured. The electron spectrometers consist of a pair of magnets producing a uniform magnetic field equal to 800 G (experiment B) or 1700 G (experiment A). An electron describes a circular trajectory inside the spectrometer proportional to its momentum. The 7 mm entrance hole of the spectrometer is covered by a 9 μm thick aluminum foil which protects the detectors against the light. The electron spectrometer is located 15 cm from the plasma, giving an acceptance solid angle of $\Delta\Omega = 1.7 \times 10^{-3}$ sr. Electrons are detected directly in the focal plane of the spectrometer by six thick silicon diodes. Each electron of energy W creates $W_{eV}/3.66$ pairs of electron-hole in the depletion region of the silicon. To make sure that the signal is actually due to electrons, we made null tests by inverting the magnetic field direction, or by closing the spectrometer with a 5 mm thick glass filter to stop all the electrons. In both cases, we observed a weak noise level. To avoid x rays and electromagnetic noises, diodes are protected with a 5 mm thick piece of lead inserted between the plasma and the diodes, all the coaxial cables are screened, and the six oscilloscopes have been set in a Faraday chamber.

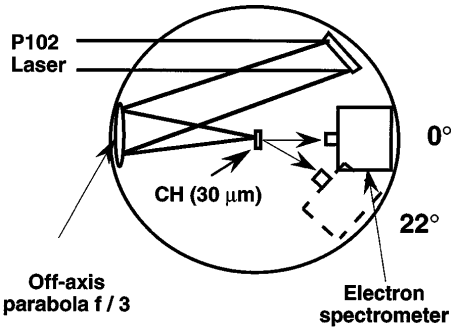

FIG. 1. Experimental setup A. The 0.4–3 MeV spectrometer ($B = 1700$ G) is used to measure the electrons ejected from a 30 μm thick CH target. The observation angles are equal to 0° and 22° in the forward direction. The laser beam irradiates the target at normal incidence with a maximum intensity equal to 2×10^{19} W/cm^2.

Figures 2(a) and 2(b) show, respectively, typical electron distributions measured at 0° and 22° of the laser axis in the forward direction. The laser irradiates normally a 30 μm thick CH target. The data can be fit by a Boltzmann distribution, $f(W) \sim \exp(-W/kT_h)$. For 9×10^{18}, 3×10^{18}, and 2×10^{18} W/cm^2 laser intensities, the hot temperatures at 0° are, respectively, 891, 420, and 374 keV. For 9.8×10^{18} and 2×10^{18} W/cm^2 laser intensities, the hot temperatures at 22° are, respectively, 724 and 440 keV. We present in Fig. 3 the evolution of the hot temperature versus the laser intensity. The hot temperatures along the laser propagation axis [Fig. 3(a)] and at 22° to this axis in the forward direction [Fig. 3(b)] are much larger than the temperatures of the 135° emission [Fig. 3(b)].

In Fig. 3(a) the curve line is the function $T_h(\text{MeV}) = 0.511[(1 + I_{18}/1.37)^{1/2} - 1]$. The experimental data are well localized around this curve. The hot temperature evolution versus the laser intensity of the electrons ejected along the laser axis in the forward direction is

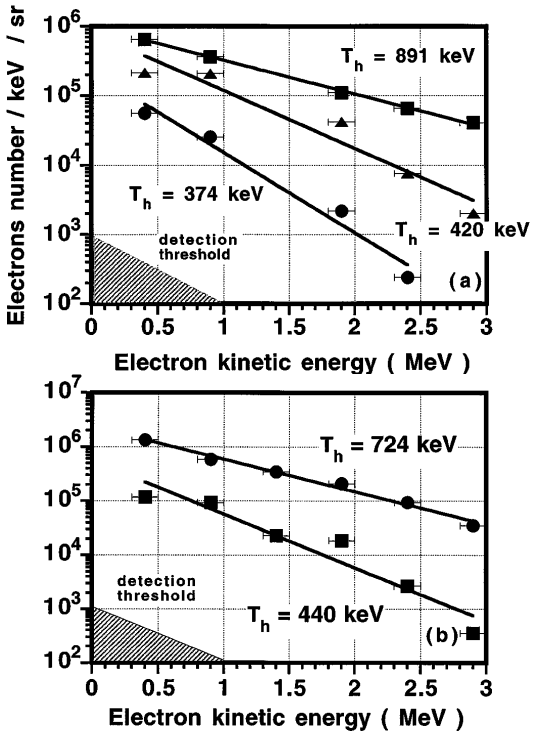

FIG. 2. (a) Electron distributions from 0.4 to 3 MeV, for 9×10^{18}, 3×10^{18}, and 2×10^{18} W/cm^2 laser intensities, measured along the laser propagation axis in the forward direction. Hot temperatures are, respectively, 891, 420, and 374 keV, assuming a Boltzmann distribution $f(W) = dN/dW \sim \exp(-W/kT_h)$ (solid lines). The vertical axis gives the electron number by units of keV and steradian. The horizontal bar represents the spectral width, i.e., the spatial extension of the diodes. (b) Electron distributions from 0.4 to 3 meV, for 9.8×10^{18}, and 2×10^{18} W/cm^2 laser intensities, measured at 22° in the forward direction. Hot temperatures are, respectively, 724 and 440 keV.

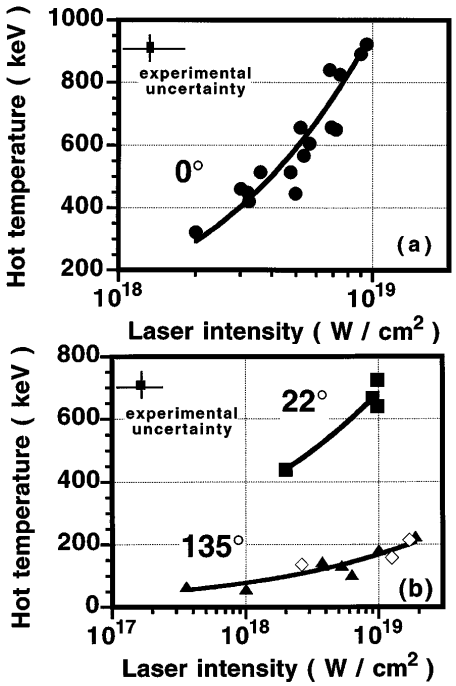

FIG. 3. Hot temperature versus the laser intensity: (a) For the electrons ejected along the laser propagation axis in the forward direction (circles), the evolution law of the hot temperature is in agreement with the model given by Wilks *et al.* [4], the curve line showing the fit $T_h(\mathrm{MeV}) = 0.511[(1 + I_{18}/1.37)^{1/2} - 1]$. (b) For the electrons ejected at 22° to this axis in the forward direction (square) and at 135° in the backward direction (triangle, p polarization; diamond, s polarization); curve lines show fits scaling as I^a (with $a \sim 0.33$ and $a \sim 0.28$ for, respectively, the 135° and 22° emission).

in good agreement with the model introduced by Wilks *et al.* [4], where $T_h = (\gamma_{\mathrm{osc}} - 1)mc^2$. These results suggest that the electrons oscillating in the laser electric field are ejected longitudinally by a strong magnetic field (>100 MG) in a distance shorter than the laser wavelength. The interaction of the subpicosecond pulse is then supposed to be localized in the overdense region of a steepened density gradient plasma [14]. The hot temperature for the other observation angles scale as I^a, with $a \sim 0.33$ for the 135° emission, and $a \sim 0.28$ for the 22° emission, which suggests other mechanisms in these directions.

The efficiency of hot electron production η versus the laser energy, defined as the ratio of the total energy in the hot electrons to the laser energy contained in the focal spot, is presented in Fig. 4. There is no large difference in the efficiency for the three observations: It reaches 0.1%/sr. Assuming isotropic distribution, 1% of the laser energy is transferred into hot electrons escaping from the target. In more recent experiments, we have changed the 30 μm thick CH target to 0.3 and 0.7 μm thick CH targets, and 0.7 and 1.5 μm thick Al targets. The laser irradiated the target at 0° incidence at 10^{19} W/cm^2. The number of MeV electrons detected along the laser propagation axis in the forward direction sharply increased (×30). We have changed the entrance of the spectrometer to a smaller

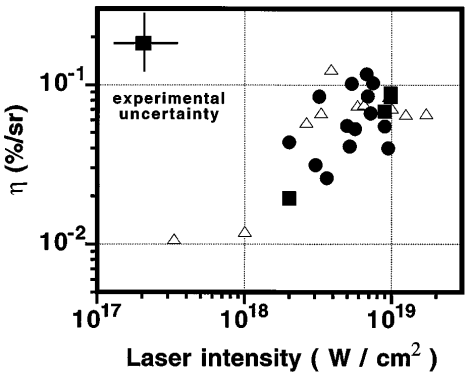

FIG. 4. Efficiency η by steradian of hot electron production versus the laser intensity. It reaches 0.1%/sr for the three observations (circle, 0° emission; square, 22° emission; triangle, 135° emission).

one. We measure an efficiency of 3%/sr, and, assuming isotropic emission, more than 30% of the laser energy is transferred into hot electrons.

In summary, we have performed the first experiments to investigate the interaction of ultraintense $I\lambda^2 > 10^{19}\ \mathrm{W/cm^2}\ \mu\mathrm{m}^2$ subpicosecond laser pulses with a solid target. We have investigated the coupling of laser energy to energetic escaping electrons from 0.06 to 3 MeV. These observations exhibit Boltzmann distributions with different scaling laws of the hot temperature versus the laser intensity. The hot temperature scale law of the 0° emission is in very good quantitative agreement with the model given by Wilks *et al.* [4], where $T_h = (\gamma_{\mathrm{osc}} - 1)mc^2$. The hot temperature reaches 1 MeV at a $10^{19}\ \mathrm{W/cm^2}$ laser intensity. Electrons are accelerated along the laser propagation axis in the forward direction by the laser ponderomotive potential, and ejected by the $\mathbf{V} \times \mathbf{B}$ component of the Lorentz force, in a steepened density profile. More than 3%/sr of the laser energy is converted into hot electrons.

We would like to thank F. Amiranoff, G. Bonnaud, M. Busquet, D. Juraszek, E. Lefebvre, M. Louis-Jacquet, G. Mainfray, V. Malka, G. Nierat, and C. Rousseaux for fruitful discussions. We also wish to acknowledge encouragement and support from M. Decroisette and A. Jolas as well as the technical assistance of the P102–Castor staff at CEA Limeil.

[1] C. Darrow, S. Lane, D. Klem, and M. D. Perry, SPIE **1860** (1993).

[2] A. Modena, Z. Najmudin, A. E. Dangor, C. E. Clayton, K. A. Marsh, C. Joshi, V. Malka, C. B. Darrow, C. Danson, D. Neely, and F. N. Walsh, Nature (London) **377**, 606 (1995).

[3] M. Tabak, J. Hammer, M. E. Glinsky, W. L. Kruer, S. C. Wilks, J. Woodworth, E. M. Campbell, and M. D. Perry, Phys. Plasmas **1**, 1626 (1994).

[4] S. C. Wilks, W. L. Kruer, M. Tabak, and A. Langdon, Phys. Rev. Lett. **69**, 1383 (1992); *The Physics of Laser Plasma Interactions*, edited by W. L. Kruer (Addison-Wesley, Redwood City, 1988).

[5] N. H. Ebrahim, H. A. Baldis, C. Joshi, and R. Benech, Phys. Rev. Lett. **45**, 1179 (1980); F. Brunel, Phys. Rev. Lett. **59**, 52 (1987).

[6] K. Estabrook and W. L. Kruer, Phys. Fluids **26**, 7 (1983).

[7] C. Rousseaux, G. Malka, J. L. Miquel, F. Amiranoff, S. D. Baton, and Ph. Mounaix, Phys. Rev. Lett. **74**, 23 (1995).

[8] P. Monot, T. Auguste, P. Gibbon, F. Jakober, G. Mainfray, A. Dulieu, M. Louis-Jacquet, G. Malka, and J. L. Miquel, Phys. Rev. Lett. **74**, 15 (1995); C. E. Max, J. Arons, and A. B. Langdon, Phys. Rev. Lett. **33**, 209 (1974); P. Sprangle, C. M. Tang, and E. Easarey, IEEE Trans. Plasma Sci. **15**, 145 (1987); G. Z. Sun, E. Ott, Y. C. Lee, and P. Guzdar, Phys. Fluids **30**, 526 (1987); H. S. Brandi *et al.*, Phys. Fluids **5**, 3539 (1993).

[9] A. P. Fews, P. A. Norreys, F. N. Beg, A. R. Bell, A. E. Dangor, C. N. Danson, P. Lee, and S. J. Rose, Phys. Rev. Lett. **73**, 1801 (1994).

[10] M. Schnürer, M. P. Kalashnikov, P. V. Nickles, Th. Schlegel, W. Sandner, M. Demchenko, R. Nolte, and P. Ambrosi, Phys. Plasmas **2**, 8 (1995); J. D. Kmetec, C. L. Gordon, III, J. J. Macklin, B. E. Lemoff, G. S. Brown, and S. E. Harris, Phys. Rev. Lett. **68**, 1527 (1992).

[11] O. Peyrusse, M. Busquet, J. C. Kieffer, Z. Jiang, and C. Y. Côté, Phys. Rev. Lett. **75**, 3862 (1995).

[12] N. Blanchot, C. Rouyer, S. Sauteret, and A. Migus, Opt. Lett. **20**, (1995).

[13] S. Jacquemot and A. Decoster, Laser Part. Beams **9**, 517 (1991).

[14] E. G. Gamaly, Phys. Fluids B **5**, 10 (1993); F. V. Hartemann, S. N. Fochs, G. P. Le Sage, N. C. Luhmann, Jr., J. G. Woodworth, M. D. Perry, Y. J. Chen, and A. K. Kerman, Phys. Rev. E **51**, 4833 (1995); M. E. Glinsky, Phys. Plasmas **2**, 7 (1995); P. Gibbon, Phys. Rev. Lett. **73**, 664 (1994); J. Denavit, Phys. Rev. Lett. **69**, 3052 (1992).